Optical excitation in the creep phase of plastic charge-density waves

Naoki Ogawa and Kenjiro Miyano
Research Center for Advanced Science and Technology, University of Tokyo, Tokyo 153-8904, Japan

Serguei Brazovski
Laboratoire de Physique Theorique et Modeles Statistiques, CNRS Bat.100, Universite Paris-Sud, 91405 Orsay-Cedex France
(Received 9 July 2004; revised manuscript received 29 November 2004; published 28 February 2005)

Creep motion of the charge-density wave (CDW) and its change through optical excitation in the low-temperature plastic state of $K_{0.3}MoO_3$ is analyzed in terms of a local pinning theory. The nonlinear *I-V* curve below the sliding threshold field can be well reproduced with a numerical calculation, and it is shown that photoexcitation increases the transition probability of phase slips, which promotes the creep motion, and also leads to a relaxation of the phase strain. Photoexcitation can offer an effective method to control the dynamics of CDW through this deformation manipulation.

DOI: 10.1103/PhysRevB.71.075118 PACS number(s): 71.45.Lr, 72.15.Nj, 78.20.−e

I. INTRODUCTION

Many sliding charge-density wave (CDW) materials,[1–5] including fully gapped $K_{0.3}MoO_3$, TaS_3, and partially gapped $NbSe_3$, show dramatic changes in their transport properties at low temperatures, such as freezing out of relaxation time and appearance of a second sliding threshold, indicating a qualitative modification of the pinned state of the CDW[6–9] (see Ref. 10 for a review). These changes in the CDW dynamics[11,12] are characterized by interactions between collective pinning, local pinning, Coulomb interaction,[13] and thermal fluctuation.[14] A typical CDW conductor $K_{0.3}MoO_3$ shows a Peierls transition at $T_p \sim 183$ K and becomes semiconducting due to nearly perfect nesting of its Fermi surface. Slightly below T_p, the current is carried by thermally activated normal carriers and also by the collective motion of the CDW. Ohmic conduction can be observed above ~ 50 K with small bias voltage, and the current follows a power law with respect to voltage down to ~ 30 K.[15] A second threshold in the *I-V* curve appears below ~ 25 K, sometimes accompanied by a discontinuity (called switching) with hysteresis, and becomes pronounced with decreasing temperature. Between two thresholds, the current increases nearly exponentially with applied voltage, and is temperature activated with an activation energy comparable to the Peierls gap. These dynamics have also been discussed in terms of the dynamic phase transitions from the analogue of vortex lattices.[16] Although the origin of the switching is not clearly understood at this moment, the low-temperature phase have been ascribed to the plastic (or glass-like) state of the CDW,[11] dominated by local (strong) pinnings after the freezing out of normal carriers that screen the CDW deformations at higher temperatures. The local pinning is characterized by a relatively small barrier height that can be overcome even at low temperatures, while the collective (weak) elastic pinning induces a large barrier height [$\sim 10^3 k_B T_p$ (Ref. 10)] and dominates the high-temperature elastic regime. The relaxation of these two processes shows a crossover around 23 K,[11] and the first threshold disappears because it is inversely proportional to the CDW elastic constant,[17] whose longitudinal component $C_{\|} \sim 1/\rho_n$ diverges with the disappearance of normal carrier density $\rho_n \sim \exp(-\Delta/T)$.

Recently, Lemay *et al.* reported that the creep motion of the CDW in $NbSe_3$ can be monitored through narrow-band noise,[18] indicating its temporally ordered collective motion, and the creep current can be expressed as

$$J_c(E,T) = \sigma_0(E - E_T)\exp\left(-\frac{T_{pin}}{T}\right)\exp\left(\alpha\frac{E}{T}\right), \qquad (1)$$

where E_T is a threshold field, T_{pin} is pinning strength, E is an external electric field, and α is a constant. Equation (1) shows a thermally assisted flux creep[19] and resembles the field-assisted hopping conduction,[20] although the prefactor linear to the electric field is added phenomenologically. Although *I-V* curves in the creep regime of $K_{0.3}MoO_3$ can also be fitted with Eq. (1),[21] the conclusive theory for the transport properties in the low-temperature phase has been awaited.

A local pinning approach to the time-dependent properties of plastic sliding density waves, in terms of local metastable states created by pinning-induced solitons or dislocation loops (see Ref. 22 for a review), has been developed recently,[14] in which the CDW is considered as an elastic periodic medium with topological defects interacting with impurities.[23] This theory can describe anomalous peaks in temperature and frequency-dependent dielectric susceptibility $\epsilon(T,w)$, and the appearance of the second threshold observed at low temperatures.[11,24] At these temperatures, CDW is assumed to advance with phase slips and breaking of the phase coherence.

A phase slip process occurs in many condensed matters with complex order parameters.[25] In the sliding CDW systems, when the external field is increased, strongly pinned domains are not dislodged; instead, the elastic cost of the phase deformation drives the CDW amplitude toward zero. In the optical conductivity measurement, a decrease in the spectral weight for the amplitude mode under the sliding motion has been reported.[26] Phase slips generate topological defects in the CDW, as 2π solitons in one dimension and dislocation loops in higher dimensions, which climb in the crystal and allow the CDW to progress.[27] These phase slip

processes are indispensable in the conversion between collective and normal carriers at the contacts, the temperature variation of the CDW wave vector, and the depinning of the localized regions in large samples. In the latter case, the shear deformation of the CDW phase also plays a crucial role.[28] Thus, the sliding state in the samples with a large cross section is essentially inhomogeneous,[29–31] although highly correlated motion has been predicted from the viewpoint of the dynamic phase transition, and there are some experiments showing the increase of in-chain correlation in the sliding state.[32] The interaction between topological defects with plastic and elastic deformations makes it difficult to picture the sliding state of the CDW in real space.

In this paper, we combine *I-V* measurements of $K_{0.3}MoO_3$ with optical excitation and try to explain the creep motion and its illumination intensity dependence using the local pinning theory.[14] Since the CDW is a condensation of electron-hole pairs, one can expect excitation of the quasiparticles above the Peierls gap through photoillumination. This process causes a temporary reduction of the CDW amplitude and also leads to the amplitude- and phase-mode collective excitation, which may result in the redistribution of the CDW phase. Consequently, photoexcitation can effectively induce a relaxation of phase strain.[33] Furthermore, the light illumination can also control the CDW motion because it shows sensitive dependence on the phase deformation. Note that this effect is distinct from the modulation of the CDW creep motion by the presence of free carriers, e.g., screening and back flow. One might suspect that it is difficult to differentiate the effect by thermally generated normal carriers from that by the optically generated quasiparticles. However, the lifetime of the photoexcited single particles is too short (<1 ps) to make a significant contribution as free carriers.[34] A detailed discussion about the photoeffect on the dynamics of CDW is reported elsewhere.[35] That the photocurrent is indeed very small, reflecting the short lifetime, has been reported recently in TaS_3.[36]

We note that optical effects can also be discussed in terms of the solitons—nonlinear deformations of the CDW resulting from self-trapping of electrons (see Ref. 37 for a review). It is particularly important that relaxed particles do not stay near gap edges $\pm\Delta$ as semiconductor-like electrons and holes. Instead, they acquire a form of the amplitude soliton (AS) $\sim\tanh(x/\xi_0)$, $\xi_0=\hbar v_F/\Delta$, with a smaller energy $2\Delta/\pi$.[38,39] With the amplitude passing through zero, the AS becomes a static phase slip center, thus playing a key role in effects of depinning. As well registered in conducting polymers,[40] the solitons in the optical measurements have been searched in CDWs,[41] while still without conclusive results.[42] There is some indirect evidence, such as mysterious activation energies at about 0.65Δ,[34,43] which is close to the theoretical value $2\Delta/\pi$, and the appearance of hopping-like conduction at low temperatures. The fast relaxation of optically injected carriers can be partly explained by the self-trapping of electrons into solitons.

Notice that we define solitons or their pairs as locally stable finite perturbations of one chain with respect to its neighbors. This definition is appropriate to incommensurate CDWs and corresponds to a more general notion of dislocation loops: the 2π soliton is just the elementary loop embracing one chain. This definition differs from a more traditional view of solitons as walls between distinctly different domains, which is appropriate to commensurate CDWs. In addition, our definition of phase slips is somehow broader than the most common one, while it keeps the most important ingredients. Namely, the phase slip is the instantaneous process of changing the on-chain configuration of the CDW when it gains or skips one period, $\pm 2\pi$. We allow for phase slips to take place locally, at the pinning site with a distribution over some interval terminated by divergent solitons; this process conserves the number of particles. Usually, the phase slip is interpreted more narrowly: the gain of 2π is distributed over the whole chain, which changes the total number of periods in the ground state by one, hence, the number of particles is changed by 2.

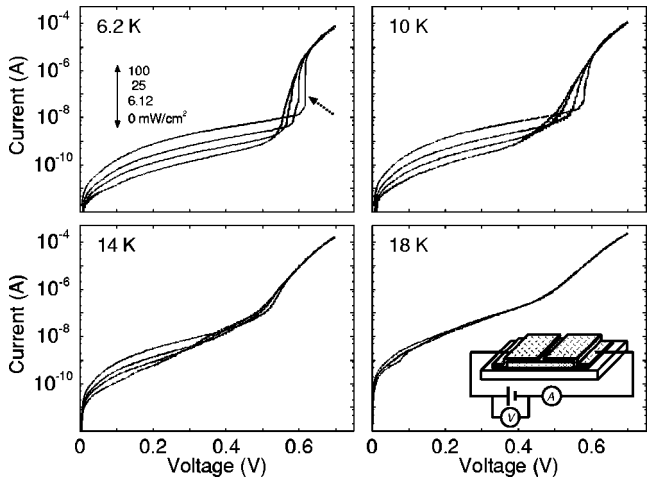

FIG. 1. Temperature and illumination intensity dependence of the *I-V* curves at low temperatures. Illumination intensity was increased as 0, 6.12, 25, and 100 mW/cm^2. Dashed arrow indicates the recovery of switching transition through illumination. Inset shows the contact arrangement.

II. MEASUREMENTS AND FITTINGS

A. Experimental setup

Sample crystals were synthesized by means of the electrolytic reduction of $KMoO_4$-MoO_3 melt.[44] Typical sample size is $1.3\times1\times0.2$ mm^3 after the cleavage. The samples were glued to sapphire plates and indium electrodes separated by 50 μm were evaporated onto the surface (Fig. 1 inset). The measurements have been performed with two-probe geometry in the crystalline *b* direction at low temperatures (<25 K).

We used a cw laser of 2.33eV ($\lambda=532$ nm) as a light source, whose penetration depth is about 100 nm (Ref. 45)—much smaller than the sample thickness. However, considering the large anisotropy of conductivity and electrode geometry, the creep and sliding motion should start near the sample surface, assuring the effectiveness of the photoexcitation (details on the distributions of current are given in the Appendix). The light spot covers the whole sample surface, including the electrodes. The electrodes are opaque and light

focused on them shows no effect in the transport. We note that the photoeffects could be observed only with the incident photons with their energy exceeding the Peierls gap, and are qualitatively similar for photons with energy in the visible and near-infrared range.[21]

B. *I-V* characteristics

Figure 1 shows the temperature and illumination intensity dependence of *I-V* curves. In the dark at 6.2 K, the current starts nearly linearly with applied voltage, shows exponential increase between 0.2 and 0.5 V, and finally reaches the second threshold voltage V_s. As discussed above, the first threshold cannot be well defined at these temperatures. With light illumination, the creep current and the sliding threshold V_s increase in response to light intensity. The rounding of the *I-V* curve at V_s in the dark could be due to the size effects.[28,46] The photoinduced recovery of the clear switching transition (at 6.2 K in Fig. 1) is one of the obvious features of the photoexcitation.[35] When temperature is increased, the photoinduced growth of the creep current and also the shift of V_s become small. At 18 K, the photoeffect becomes barely discernible, and seen only at low bias. The temperature range in which clear sliding transition and large photoeffects can be observed, well coincides with that in which the glass-like behavior dominates, as observed, e.g., in dielectric susceptibility measurements.[47] We have interpreted the above effects as follows: incident photons excite the electrons in the CDW above the Peierls gap. Excited quasiparticles instantly recondense into a less deformed phase configuration, accompanied by effective phase slips and annealing of phase defects. In the former case, the photoexcitation enhances a creep motion, and in the latter, it shifts the breaking transition of the CDW to a higher bias voltage by partially recovering the phase coherence. The persistence of the photoexcitation effect[48] augments this picture. Since CDW motion starts near the surface in our geometry, photocontrol of the CDW within the penetration depth has an impact on the entire CDW motion through shear deformation[28] and gliding of phase dislocations, although it is difficult to say how deep in the sample the CDW moves at this moment.

C. Local pinning approach

The Hamiltonian for the elastic density waves interacting with randomly distributed pinning potential can be expressed as

$$H = \int_D d^d x \left(\frac{C}{2} [\nabla \varphi(\boldsymbol{x})]^2 + \sum_i V_{pin,i} \{1 - \cos[\boldsymbol{Q} \cdot \boldsymbol{x} + \varphi(\boldsymbol{x})]\} \times \delta(\boldsymbol{x} - \boldsymbol{x}_i) \right), \tag{2}$$

where D represents a volume covering the collective pinning domain, C is an elastic constant of the density wave, and $\boldsymbol{Q}$ is a wave vector. The first term in Eq. (2) represents the elastic energy, which cannot grow unlimitedly for a moving CDW. Considering a very strong point impurity and a periodic nature of the density wave, the large elastic deformation should be released by nucleation of phase defects as phase solitons or dislocation loops,[49] yielding a large number of metastable states. This process starts with a phase slip and repeats periodically; the CDW deformation at a pinning site exceeds a critical value, which leads to local suppression of the order parameter, and finally to destruction of the CDW phase coherence and removal of the accumulated phase difference by 2π [Fig. 2(a)].

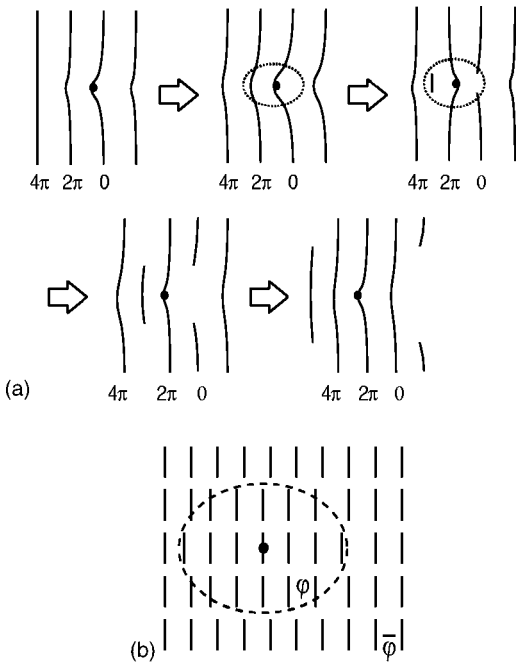

FIG. 2. (a) Phase slip process and growing dislocations in the CDW. The crests of the wave fronts are marked by the solid lines. If the CDW phase deformation exceeds π with respect to its original configuration, the system becomes bistable, and then a phase slip occurs. This process repeats periodically. (b) Definition of the local variables. The filled circle shows a pinning potential and the dotted line represents a pinning domain.

Let us consider a single pinning site located at $\boldsymbol{x}_i$. The deformation energy [the first term in Eq. (2)] can be obtained by minimizing it for a given phase at the pinning site, $\varphi(\boldsymbol{x}_i)$, when the deformation is small. A realistic calculation, however, is difficult for a large deformation, in which the creation of solitons has to be taken into account. The minimal model,[14] taking into account a periodicity of the interchain interaction, yields for the deformation energy

$$W(\psi_i) = E_s[1 - \cos(\psi_i/2)], \tag{3}$$

where $\psi_i = \varphi(\boldsymbol{x}_i) - \bar{\varphi}$ is the mismatch between the local phase $\varphi(\boldsymbol{x}_i)$ and the phase $\bar{\varphi}$ far away from the pinning site, representing the overall advance of the CDW (when static $\bar{\varphi}$ = const and sliding $\bar{\varphi} = -vt$). Equation (3) satisfies minimal conditions that $W(\psi)$ should satisfy: (1) quadratic with respect to ψ for a small ψ, (2) periodic in ψ, and (3) always positive. Considering a single pinning site and defining $\theta_i = -\boldsymbol{Q} \cdot \boldsymbol{x}_i - \bar{\varphi}$, one arrives at an effective Hamiltonian,

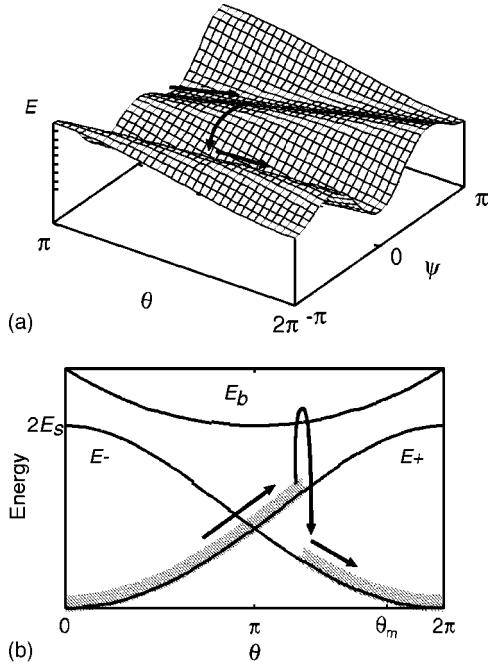

FIG. 3. (a) An example of the potential landscape. Arrows express the trajectory of the system. (b) Projection of the energy landscape in the ψ direction. When the system climbs the slope on E_+ branch with a constant velocity $\dot{\theta}$, the potential energy increases and the energy gap decreases gradually. A transition to the E_- branch then occurs.

$$H(\psi,\theta) = W(\psi) + V_{pin}(\psi-\theta), \tag{4}$$

which replaces Eq. (2), showing the competition between the cost of soliton generation and elastic deformation. The index i is omitted hereafter. Now, $2E_s$ equals the energy absorbed in the nucleation of the pair of solitons each time when ψ acquires the integer increment of 2π, and $V(\psi-\theta)=V_{pin}[1-\cos(\psi-\theta)]$ is the pinning potential. The definition of the local variables is shown in Fig. 2(b). In the presence of pinning, the CDW deforms within a certain distance from the pin (collective pinning domain), and the domain couples elastically or plastically with the surrounding phases. $H(\psi,\theta)$ should be minimized with respect to ψ at a given θ. The minima and maxima of the variational energy $H(\psi,\theta)$ determine three branches of the energy trace, E_+, E_-, and E_b. An example of the potential landscape is shown in Fig. 3(a). For a large V_{pin}, the phase ψ follows θ closely. When ψ exceeds π, a state with the CDW stepped ahead by one wavelength becomes absolutely stable, and a transition occurs overcoming the energy barrier E_b for the phase slip or the dislocation generation. The phase value θ at which the transition actually takes place depends on the velocity of the CDW as will be shown below.

If the state is monitored by θ, the evolution of the state can be traced as illustrated in Fig. 3(b). At $\theta=0$, the system is on the E_+ branch. When θ increases and exceeds π, the E_+ branch becomes metastable, and the E_- branch is now absolutely stable. The system then undergoes a transition through a local barrier E_b [activation energy: $E_b(\theta)-E_+(\theta)$], releasing the dissipation energy $\Delta E(\theta)=E_+(\theta)-E_-(\theta)$.

Let us consider a density wave moving at a constant phase velocity $v=\dot{\theta}$ and evaluate the external force $f(v)$ necessary to maintain the motion. When the density wave is deformed to θ, the fractional force exerted by the constant upward motion over the potential hill is the slope $F(\theta)[=d\Delta E(\theta)/d\theta]$ times the probability that the system *does not* switch to the E_- branch before reaching θ. For a stationary motion, the occupation number of each branch $\{n_\pm=\frac{1}{2}[1\pm n(\theta,t)]$, with $\partial n/\partial t=0\}$ obeys the kinetic equation

$$\frac{dn}{dt} = v\frac{\partial n}{\partial \theta} = \frac{n_{eq}-n}{\tau(\theta)}, \tag{5}$$

where n_{eq} is the value of n in thermal equilibrium. $f(v)$ is thus expressed as

$$f(v) \sim \int_{\pi}^{2\pi} d\theta F(\theta) n(\theta) \sim \int_{\pi}^{2\pi} d\theta F(\theta) \exp\left(-\int_{\pi}^{\theta} \frac{d\theta_1}{v\tau(\theta_1)}\right), \tag{6}$$

$$\tau(\theta) = \tau_0 \exp\left(\frac{E_g(\theta)-E_+(\theta)}{k_B T}\right), \tag{7}$$

where $\tau(\theta)$ is the rate of internal relaxation at θ, and τ_0^{-1} is an attempt rate. The activated behavior usually seen in the experiments is incorporated, as can be seen in Eq. (7). The creep-to-slide transition occurs when the shortest lifetime of the system is achieved with increasing the phase velocity $v=\dot{\theta}$. More details on this derivation and on various regimes are found in Ref. 22.

Here we shall underline only the most important regimes. The initial linear law $f\sim v$ corresponds to velocities so low that only small displacements $\delta\theta=\theta-\pi\sim\tau_\pi v\ll 1$ are effectively allowed after the branch has changed its character to become metastable. At higher v we arrive at the regime $f\sim\ln(v)$, when a wider, while still restricted, region of $\delta\theta$ is explored and the metastable branch starts to feel the decrease of the barrier (Fig. 3, there is a minimal barrier point θ_m, even if unreachable yet at these moderate v). These two regimes are covered qualitatively by the empirical formula Eq. (1). Moreover, at even higher v, the above calculations lead us to the third regime: the saturation of the pinning force at f_{max} approached as $f\approx f_{max}-\text{const}/v$. It is seen as a sharp upturn of $v(f)$ at higher f. At these high v, the metastable branch is followed as a whole, with a negligible probability to relax before the full 2π circle is complete. The cost is to create each time a pair of solitons which, being trapped or aggregated into growing dislocation loops, provide the longest relaxation time and can be an origin of the hysteresis. The photoassisted relaxation of the states created only in the high v regime can explain the observed optical memory effects.

D. Comparison with experiments

With appropriate scalings, we can evaluate Eq. (6) and compare it with the experimentally measured *I-V* characteristics. The result is shown in Fig. 4 (the lowest open circles). The absolute value of τ_0 is closely related to V_{pin} and v. We

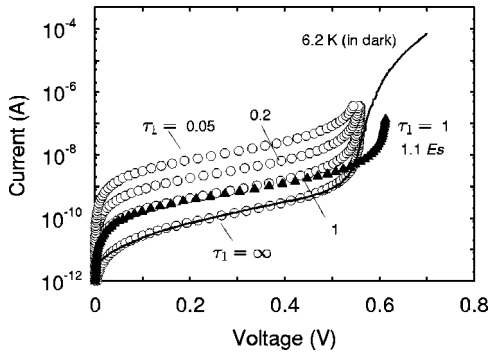

FIG. 4. Fitting of the *I-V* curve measured at 6.2 K in the dark with numerical integrations of Eq. (6) (the lowest trace of circles, labeled as "$\tau_1 = \infty$"), and its τ_1 dependence. Filled triangles show the effect of E_s on the threshold field.

assume V_{pin}=2 meV (~23 K~ crossover temperature[11]) in the following and τ_0=0.02 s so as to reproduce the temperature dependence of the *I-V* curves, which defines the unit of v. The numerical calculation compares well with the experimental data in the current range of 4 orders of magnitude covering three different regimes of sliding: linear, exponential, and the final nearly critical upturn. The deduced value of E_s (1 meV~12 K) in the dark at 6.2 K is comparable to the estimated energy of dislocation multiplication,[51] and v ~0.24 Hz at the current of 10^{-10} A in Fig. 4 is on the same order of the experimentally observed creep speed of the CDW at these temperatures and is also comparable to the creep motion reported in Ref. 18.

The effect of the optical excitation can be incorporated by adding another relaxation rate, as

$$\frac{1}{\tau(\theta)} \rightarrow \frac{1}{\tau(\theta)} + \frac{1}{\tau_1}, \tag{8}$$

where $1/\tau_1$ represents an optically induced phase slip or stress relaxation in the same scale with τ_0. The τ_1 dependence of the *I-V* curve is also shown in Fig. 4. The nearly linear offsets of the *I-V* curves with illumination intensity in logarithmic scale [Fig. 1(a)] are well reproduced. The illumination intensity (which should be proportional to $1/\tau_1$) dependence of the creep current (at 0.3 V in Fig. 4) is also evaluated, as shown in Fig. 5(b). The current increases

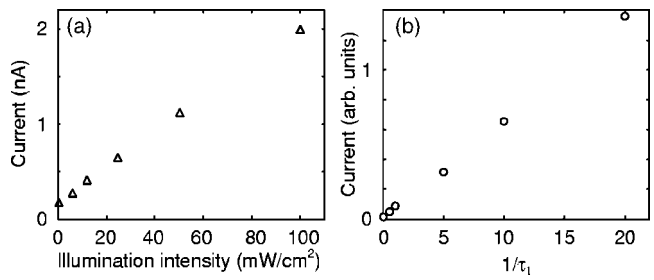

FIG. 5. (a) Illumination intensity dependence of the creep current at 6.2 K with bias voltage of 0.3 V, and (b) increase of the creep current through the optically induced transition rate $1/\tau_1$ ($\propto$ illumination intensity).

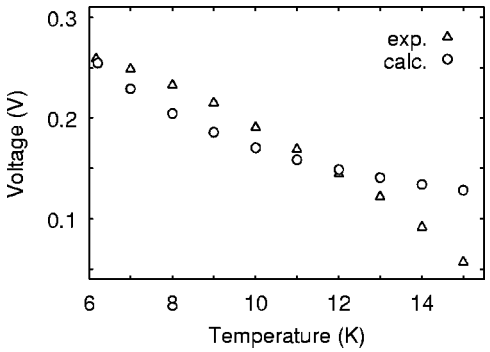

FIG. 6. Temperature dependence of the voltage to push the CDW at a constant velocity of 10^{-10} A in comparison with the numerical data of Eq. (6). The experimental data were measured in the dark ($\tau_1 = \infty$) and numerical data are scaled with the same factor as in Fig. 4.

linearly with $1/\tau_1$, which is in good agreement with the experimental data, as shown in Fig. 5(a). At illumination intensity of 100 mW/cm^2, which corresponds to 1.6 photons/s/(Mo site), the velocity of the CDW increases about 13 times over that in the dark.

Figure 6 shows the temperature dependence of the external force necessary to keep the CDW moving at a constant velocity of 10^{-10} A, which is in the $f \sim \ln(v)$ regime for all the temperatures shown in the figure. In the numerical calculation, the same scale factor as in Fig. 4 has been used. The calculation compares well with the experimental data at low temperatures and begins to deviate around 12 K ($\sim E_s$), probably due to the appearance of metastable states from the collective pinning, whose contribution should increase at higher T following the onset of screening, and also to the decrease in the sliding volume.[50]

In Fig. 7, we show the illumination intensity dependence of the external force at a constant CDW velocity of 10^{-10} A normalized with the voltage in the dark at each temperature. The data below 12 K trace the same curve, indicating that the photoeffects can be separated from the temperature effects, as is implied in the additivity rule [Eq. (8)]. Thus, the optical excitation induces an *additional* relaxation of the phase deformation, and the local pinning model can be applied at relatively low temperatures.

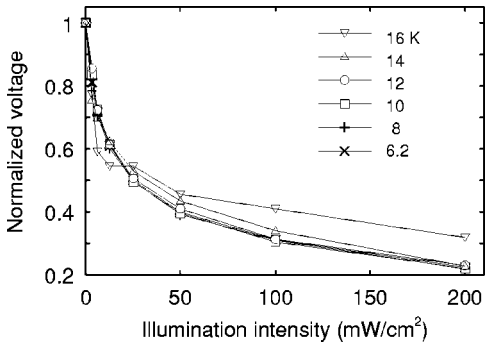

FIG. 7. Illumination intensity dependence of the voltage necessary to push the CDW at a constant velocity of 10^{-10} A normalized with the voltage in the dark.

In the local pinning model, the creep-to-slide threshold voltage is determined by the nucleation energy E_s. The photoinduced increase of the sliding threshold can be simulated by increasing E_s, as can be seen in Fig. 4. We interpret this result as the continuous repair of the partly ruptured CDW through optical removal of the phase deformation, which increases the threshold of defect nucleation. Although the numerical *I-V* curves can express the creep current fairly well, the switching transition is absent, because Eq. (6) has no singularity with increasing $\dot{\theta}$. This indicates that the switching is not a "local" effect; it rather results from much larger coherence of the CDW. In addition, the interactions of phase defects are not implemented in this model, such as annihilation of solitons and antisolitons produced at neighboring pinning centers, aggregation of solitons into growing dislocation loops, and change in viscous damping through the existence of a large number of dislocations. These should play important roles in the dynamics of CDW and would also be able to explain the absence of the switching transition at the threshold and the existence of substantial damping in the sliding regime of small-electrode-gap samples.[35]

III. CONCLUSION

In conclusion, the nonlinear *I-V* characteristics in the creep phase have been well expressed with a plastic motion of the CDW interacting with strong local impurity potentials. When the CDW moves, the phase defects are continuously nucleated, leading to a local metastable states and substantial dissipation. Optical excitation leads to the relaxation of these metastable states, and prevents the rupturing of the CDW phase, thus increasing both the transition probability of phase slips and the nucleation energy for the phase defects. Photoexcitation is therefore an effective method to control the internal degrees of freedom of the CDW and can elucidate the dynamics in the plastic state of the CDW after the freezing out of normal carriers.

ACKNOWLEDGMENTS

We thank N. Nagaosa, H. Matsukawa, A. Maeda, T. Tamegai, S. Kagoshima, and N. Kirova for valuable comments and discussions, and R. Kondo and H. Tamaru for technical help. This work was partly supported by JSPS Research Fellowships for Young Scientists, JSPS KAKENHI (15104006) and MEXT TOKUTEI (16076207).

APPENDIX: THE DISTRIBUTION OF CURRENT AND FIELD

Here we consider the distribution of current and field in our experimental geometry. At present, we study the regime of the rigid CDW considering only normal current. However, it will give us an understanding about when and where the CDW starts to slide. The results are extendable also to the first (low current) sliding regime, where the *I-V* curve is linear even for the collective conduction. We shall concentrate on the distributions around the slit between two electrodes (separation $l=2a\sim 50\ \mu$m). In comparison, the sample thickness is $t\sim 0.2$ mm and the width of the contacts is $2L\sim 1$ mm.

In general, normal carriers move under the gradients of the chemical potential μ, which incorporates both the electric potential Φ and the variable concentration of carriers n. However, the carrier concentration is not perturbed at large distances, so that $\mu=V$ (applied voltage). We define the anisotropy parameter as

$$\frac{\sigma_x}{\sigma_y}=A=B^2,\quad \sigma=\sqrt{\sigma_x\sigma_y}, \tag{A1}$$

where σ_x and σ_y are conductivities along the chains within the conducting layer and between layers in the depth direction, which correspond to the b and $(2a-c)$ directions for $K_{0.3}MoO_3$, respectively. The anisotropy parameter A can be arbitrarily large at low temperature for fully gapped CDWs, because of the different activation energies for conductance in two directions. For example, in the case of *o*-TaS_3, the anisotropy parameter was recently evaluated to be 10^3 around 120 K and should be larger at lower temperatures.[52] The value $A=10^4$ seems to be appropriate for $K_{0.3}MoO_3$ in our experimental condition ($\sim$10 K). The most important parameter is $B=A^{1/2}$, which is also big ($\sim$100). It defines the rescaling of coordinates to make the equation isotropic $(y/x\rightarrow By/x)$:

$$\boldsymbol{\nabla}\cdot\mathbf{j}=-\ \boldsymbol{\nabla}\ \cdot(\sigma\boldsymbol{\nabla}\mu)=0. \tag{A2}$$

In rescaled coordinates, the sample thickness t is B times enhanced, and the effective thickness Bt can be considered as infinite in comparison with other scales.

Now we need to write the solution of the Laplace equation for a potential $\Phi(x,y)$ in the upper half-plane $y\geqslant 0$ with the condition that at the boundary $y=0$ the potential takes values $\Phi(x>a,0)=V/2$ and $\Phi(x<-a,0)=-V/2$. As usual, the solution is written for the complex potential $P=\Phi+i\Psi$ as a function of the complex coordinate $z=x+iBy$. It is known to be

$$P=\Phi+i\Psi=\frac{V}{\pi}\arcsin\frac{z}{a}. \tag{A3}$$

The derivative dP/dz gives the components of electric field $E_{x,y}$ according to

$$-E_x+\frac{i}{B}E_y=\frac{V/\pi}{\sqrt{a^2-(x+iBy)^2}}. \tag{A4}$$

The field and the current diverge near the contact edges $y\rightarrow 0, x\rightarrow\pm a$. Near the contact plates away from the slot $y\rightarrow 0, |x|>a$,

$$E_x, j_x=0;\quad E_y=\frac{j_y}{\sigma_y}=\frac{\pm BV/\pi}{\sqrt{x^2-a^2}}, \tag{A5}$$

so that the current j_y emitted by distant parts, $|x|\gg a$, of contacts decreases very slowly, as $1/|x|$. The same concerns

the current density j_x on the line above the gap center $x=0$, which decays as $1/|y|$. The total current J given by Eq. (A5) diverges logarithmically as

$$J = \int_a^\infty j_y(x,0)dx = \int_0^\infty j_x(0,y)dy \approx \frac{\sigma}{\pi} V \ln\frac{L}{a}, \quad \text{(A6)}$$

where we have introduced the cutoff L on the order of the contact width. We see that the total current is distributed over a semi-ellipsoid of width $x \sim L \sim 1$ mm and depth $y \sim L/B \approx 10$ μm. However, the field and the current densities are rather low; at the characteristic ellipsoid boundary we find

$$\frac{j_x(x=0, y \approx L/B)}{j_x(x=0, y=0)} \approx \frac{a}{L} \sim 40^{-1}. \quad \text{(A7)}$$

In summary three different scales exist: (1) larger area $L \times L/B$ defined by contacts width L, where most of the current flows but at a relatively low density, (2) major active area $a \times a/B$, where the coherent sliding can start as soon as the minimal field $V/\pi a$ of this region (at $x, y=0$) exceeds the depinning threshold; and (3) singular regions near the contact edges $x = \pm a, y = 0$. Here the CDW is depinned very early but may not be able to slide from one region to another unless the condition in (2) is satisfied at a higher voltage.

[1] For a review, G. Grüner, Rev. Mod. Phys. **60**, 1129 (1988); G. Grüner, *Density Waves in Solids* (Addison-Wesley Longmans, MA, 1964).

[2] *Charge Density Waves in Solids*, edited by L. Gor'kov and G. Grüner (Elsevier, New York, 1989).

[3] *Proceedings of the International Workshop on Electronic Crystals*, Carry-le-Rouet, France, 1993, edited by S. Brazovskii and P. Monceau [J. Phys. IV **3** C2 (1993)].

[4] *Proceedings of the International Workshop on Electronic Crystals*, La Colle-sur-Loup, France, 1999, edited by S. Brazovskii and P. Monceau [J. Phys. IV **9** (1999)].

[5] *Proceedings of the International Workshop on Electronic Crystals*, St. Flour, France, 2002, edited by S. Brazovskii, N. Kirova, and P. Monceau [J. Phys. IV **12** (2002)].

[6] A. Zettl and G. Grüner, Phys. Rev. B **26**, 2298 (1982).

[7] R. M. Fleming, R. J. Cava, L. F. Schneemeyer, E. A. Rietman, and R. G. Dunn, Phys. Rev. B **33**, 5450 (1986).

[8] G. Mihaly and P. Beauchene, Solid State Commun. **63**, 911 (1987).

[9] S. Ravy, H. Requardt, D. Le Bolloc'h, P. Foury-Leylekian, J.-P. Pouget, R. Currat, P. Monceau, and M. Krisch, Phys. Rev. B **69**, 115113 (2004).

[10] R. E. Thorne, K. Cicak, K. O'Neill, and S. G. Lemay, *Proceedings of the International Workshop on Electronic Crystals*, edited by S Brazovskii, N. Kirova, and P. Monceau [J. Phys. IV **12**, 291 (2002)].

[11] D. Starešinić, K. Biljaković, W. Brütting, K. Hosseini, and P. Monceau, in *Proceedings of the International Workshop on Electronic Crystals*, edited by S. Brazovskii, N. Kirova, and P. Monceau [J. Phys. IV **12**, 15 (2002)]; D. Starešinić, K. Hosseini, W. Wrütting, K. Biljaković, E. Riedel, and S. van Smaalen, cond-mat/0309104; for a review F. Nad and P. Monceau, in *Proceedings of the International Workshop on Electronic Crystals*, edited by S. Brazovskii and P. Monceau [J. Phys. IV **3**, 343 (1993)].

[12] D. Starešinić, K. Biljaković, W. Brütting, K. Hosseini, P. Monceau, H. Berger, and F. Levy, Phys. Rev. B **65**, 165109 (2002).

[13] B. Hennion, J.-P. Pouget, and M. Sato, Phys. Rev. Lett. **68**, 2374 (1992); S. Artemenko and A. Volkov, *Charge Density Waves in Solids*, edited by L. Gor'kov and G. Grüner (Elsevier, New York, 1989).

[14] S. Brazovskii and A. Larkin, in *Proceedings of the International Workshop on Electronic Crystals*, edited by S. Brazovskii and P. Monceau [J. Phys. IV **9**, 77 (1999)]; S. Brazovskii and A. Larkin, Synth. Met. **86**, 2223 (1997); A. Larkin and S. Brazovskii, Solid State Commun. **93**, 275 (1995).

[15] G. Mihály, P. Beauchêne, J. Marcus, J. Dumas, and C. Schlenker, Phys. Rev. B **37**, 1047 (1988).

[16] L. Balents and M. P. A. Fisher, Phys. Rev. Lett. **75**, 4270 (1995).

[17] An important feature of the semiconducting CDWs is the Coulomb hardening (Ref. 13) of their compressibility when the normal carriers freeze out at low temperatures. For a review, see Ref. 10.

[18] S. G. Lemay, R. E. Thorne, Y. Li, and J. D. Brock, Phys. Rev. Lett. **83**, 2793 (1999).

[19] P. W. Anderson and Y. B. Kim, Rev. Mod. Phys. **36**, 39 (1964).

[20] R. M. Hill, Philos. Mag. **24**, 1307 (1971).

[21] N. Ogawa, A. Shiraga, R. Kondo, S. Kagoshima, and K. Miyano, Phys. Rev. Lett. **87**, 256401 (2001).

[22] S. Brazovskii and T. Nattermann, Adv. Phys. **53**, 177 (2004).

[23] J. C. Gill, Phys. Rev. B **63**, 125125 (2001).

[24] J. Yang and N. P. Ong, Phys. Rev. B **44**, 7912 (1991).

[25] P. W. Anderson, *Basic Notions of Condensed Matter Physics* (Benjamin Cummings, New York, 1984).

[26] B. Gorshunov, S. Haffner, M. Dressel, B. Lommel, F. Ritter, and W. Assmus, in *Proceedings of the International Workshop on Electronic Crystals*, edited by S. Brazovskii, N. Kirova, and P. Monceau [J. Phys. IV **12**, 81 (2002)].

[27] N. P. Ong and K. Maki, Phys. Rev. B **32**, 6582 (1985).

[28] K. O'Neill, K Cicak, and R. E. Thorne, Phys. Rev. Lett. **93**, 066601 (2004).

[29] S. G. Lemay, M. C. de Lind van Wijngaarden, T. L. Adelman, and R. E. Thorne, Phys. Rev. B **57**, 12 781 (1998); S. G. Lemay, T. L. Adelman, S. V. Zaitsev-Zotov, and R. E. Thorne in *Proceedings of the International Workshop on Electronic Crystals*, edited by S. Brazovskii and P. Monceau [J. Phys. IV **9**, 149 (1999)].

[30] S. Brazovskii and N. Kirova, in *Proceedings of the International Workshop on Electronic Crystals*, edited by S. Brazovskii and P. Monceau [J. Phys. IV **9**, 139 (1999)].

[31] H. Requardt, F. Ya. Nad', P. Monceau, R. Currat, J. E. Lorenzo, S. Brazovskii, N. Kirova, G. Grübel, and Ch. Vettier, Phys. Rev. Lett. **80**, 5631 (1998).

[32] R. Danneau, A. Ayari, D. Rideau, H. Requardt, J. E. Lorenzo, L. Ortega, P. Monceau, R. Currat, and G. Grübel, Phys. Rev. Lett. **89**, 106404 (2002).

[33] N. Ogawa, Y. Murakami, and K. Miyano, Phys. Rev. B **65**, 155107 (2002).
[34] J. Demsar, K. Biljaković, and D. Mihailovic, Phys. Rev. Lett. **83**, 800 (1999).
[35] N. Ogawa and K. Miyano, Phys. Rev. B **70**, 075111 (2004).
[36] S. V. Zaitsev-Zotov and V. E. Minakova, JETP Lett. **79**, 550 (2004).
[37] S. Brazovskii, in *Charge Density Waves in Solids*, edited by L. Gor'kov and G. Grüner (Elsevier, New York, 1989), p. 425.
[38] H. Takayama, Y. R. Lin-Liu, and K. Maki, Phys. Rev. B **21**, 2388 (1980).
[39] M. Nakano and K. Machida, Phys. Rev. B **33**, 6718 (1986).
[40] A. J. Heeger, S. Kivelson, J. R. Schrieffer, and W.-P. Su, Rev. Mod. Phys. **60**, 781 (1988).
[41] G. Minton and J. W. Brill, Phys. Rev. B **45**, 8256 (1992); R. C. Rai, V. A. Bondarenko, and J. W. Brill, Eur. J. Biochem. **35**, 233 (2003).
[42] J. W. Brill, Solid State Commun. **130**, 437 (2004).
[43] For example, D. C. Johnston, J. P. Stokes, P.-L. Hirsh, and G. Güner, J. Phys. Colloq. **C3** 1794 (1983).
[44] A. Wold, W. Kunnmann, R. J. Arnott, and A. Ferretti, Inorg. Chem. **3**, 545 (1964).
[45] L. Degiorgi, B. Alavi, G. Mihaly, and G. Grüner, Phys. Rev. B **44**, 7808 (1991).
[46] D. V. Borodin, S. V. Zaĭtsev-Zotov, and F. Ya. Nad, Sov. Phys. JETP **63**, 184 (1986).
[47] F. Ya. Nad and P. Monceau, Solid State Commun. **87**, 13 (1993); in *Proceedings of the International Workshop on Electronic Crystals*, edited by S. Brazovskii and P. Monceau [J. Phys. IV **3**, 343 (1993)].
[48] N. Ogawa and K. Miyano, Appl. Phys. Lett. **80**, 3225 (2002).
[49] D. Feinberg and J. Friedel, J. Phys. (France) **49**, 485 (1988).
[50] R. M. Fleming, R. G. Dunn, and L. F. Schneemeyer, Phys. Rev. B **31**, 4099 (1985).
[51] D. Feinberg and J. Frielel, *Low-Dimensional Electronic Properties of Molybdenum Bronzes and Oxides*, edited by C. Schlenker (Kluwer, Norwell, MA, 1989), p. 427.
[52] E. Slot, H. S. J. van der Zant, and R. E. Thorne, Phys. Rev. B **65**, 033403 (2001).